

108  
X-691-72-63

65864

# DISSOCIATIVE EXCITATION OF VACUUM ULTRAVIOLET EMISSION FEATURES BY ELECTRON IMPACT ON MOLECULAR GASES III. CO<sub>2</sub>

(NASA-TM-X-65864) DISSOCIATIVE EXCITATION  
OF VACUUM ULTRAVIOLET EMISSION FEATURES BY  
ELECTRON IMPACT ON MOLECULAR GASES. 3:

CO<sub>2</sub> M.J. Mumma, et al (NASA) Mar. 1972

37 p

N72-21676

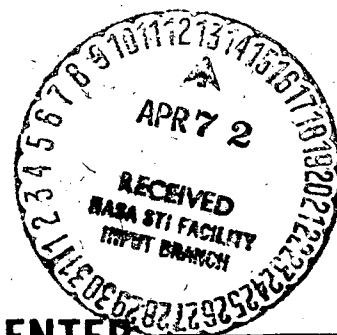
Unclass

CSCL 20H G3/24

23642

M. J. MUMMA  
W. L. BORST  
E. C. ZIPF

MARCH 1972



**GSFC**

**GODDARD SPACE FLIGHT CENTER**

**GREENBELT, MARYLAND**

PAGES-37  
CATEGORY 24

# DISSOCIATIVE EXCITATION OF VACUUM ULTRAVIOLET EMISSION

## FEATURES BY ELECTRON IMPACT ON MOLECULAR GASES<sup>\*†</sup>

### III. CO<sub>2</sub>

M. J. Mumma<sup>‡</sup>, W. L. Borst<sup>\*\*</sup>, and E. C. Zipf  
Physics Department, University of Pittsburgh  
Pittsburgh, Pennsylvania 15213

#### ABSTRACT

Vacuum ultraviolet multiplets of CI, CII, and OI have been produced by electron impact on CO<sub>2</sub>. Absolute emission cross sections for these multiplets have been measured from threshold to 350 eV. The electrostatically focussed electron gun used in this series of experiments is described in detail. The atomic multiplets which were produced by dissociative excitation of CO<sub>2</sub> and the cross sections at 100 eV are: OI(2p<sup>4</sup> <sup>3</sup>P - 2p<sup>3</sup>3s <sup>3</sup>S) 1304Å - 1.04 x 10<sup>-18</sup> cm<sup>2</sup> ± 18%; CI(2s<sup>2</sup>2p<sup>2</sup> <sup>3</sup>P - 2s2p<sup>3</sup> <sup>3</sup>P<sup>o</sup>) 1329Å - 2.67x10<sup>-19</sup> cm<sup>2</sup> ± 21%; CI(2s<sup>2</sup>2p<sup>2</sup> <sup>3</sup>P - 2s2p<sup>3</sup> <sup>3</sup>D<sup>o</sup>) 1561Å - 7.50x10<sup>-19</sup> cm<sup>2</sup> ± 30%; CI(2p<sup>2</sup> <sup>3</sup>P - 2p3s <sup>3</sup>P<sup>o</sup>) 1657Å - 1.45x10<sup>-18</sup> cm<sup>2</sup> ± 23%; CII(2s<sup>2</sup>2p <sup>2</sup>P<sup>o</sup> - 2s2p<sup>2</sup> <sup>2</sup>D) 1335Å - 7.60x10<sup>-19</sup> cm<sup>2</sup> ± 22%; and CII(2s2p<sup>2</sup> <sup>2</sup>D - 2p<sup>3</sup> <sup>2</sup>D<sup>o</sup>) 1324Å - 1.33x10<sup>-20</sup> cm<sup>2</sup> ± 23%. The dependence of the excitation functions on electron energy shows that these multiplets are produced by electric-dipole-allowed transitions in CO<sub>2</sub>.

## INTRODUCTION

In parts I and II of this series, we described dissociative excitation of atomic multiplets of HI, OI, and NI by electron impact on  $H_2$ ,  $O_2$ , and  $N_2$ , respectively.<sup>1,2</sup> Excitation of the CO fourth positive group by electron impact on CO and on  $CO_2$  was also studied.<sup>3,4</sup> In this paper we present absolute cross sections for dissociative excitation of  $CO_2$  to yield multiplets of CI, CII, and OI in the vacuum ultraviolet.

The measurements on  $CO_2$  were inspired by the then-imminent ultraviolet spectroscopic observations of the Mars upper atmosphere by the Mariner 6 and 7 spacecraft. The multiplets discussed in this paper were found to be prominent features of the Mars dayglow. Barth et al<sup>5</sup> have shown that they are produced in the Mars upper atmosphere by the action of solar photons and photoelectrons on  $CO_2$ . The cross sections presented here have been utilized by McConnell and McElroy<sup>6</sup> to perform detailed calculations of the CI 1657 Å and CI 1561 Å emissions in the dayglows of Venus and Mars.

The dissociative excitation of  $CO_2$  has been studied concurrently with this work by Ajello<sup>7</sup> and Sroka.<sup>8</sup>

## EXPERIMENT

The experiment featured an electrostatically focussed electron beam which was varied in energy from  $\sim 5$  eV to 350 eV. Photons were collected at right angles to the electron beam by a McPherson Model 225 monochromator and an EMR 541G-08-18 solar-blind photomultiplier tube. Coherent summing techniques were used to improve the statistics of the data. The experimental techniques and apparatus have been described in detail elsewhere,<sup>1,9,10</sup> with the exception of the electron gun, which we describe here.

The electron gun was electrostatically focussed<sup>11</sup> and made use of the multistage principle.<sup>12</sup> The gun configuration is shown schematically in Fig. 1. Electrons from a thorium coated iridium filament F were accelerated through an aperture in the grid G towards anode A and electrode L. The electrons were then decelerated to their final energy by the potential on electrode P and the gun housing. The collision chamber was at the same potential as the gun housing. High potentials on electrodes A and L served to reduce the space charge in front of the cathode. This yielded relatively high beam currents at low energy.

The electron gun used was a modified oscilloscope gun (Superior Electronics Corp., Model SE-2B). The modifications included a change of the aperture sizes and a different electrical mode of operation. The modified aperture sizes and potentials applied to the electrodes are listed in Table I. These potentials for the optimum focussing conditions were obtained by trial and error and are approximate. The final energy of the electrons in the collision chamber was  $eV_0$ .

For convenience, the potential on electrode L was chosen to be the same as that on A. A slightly different potential on L may result in even better focussing. All potentials were obtained from a single voltage supply by potentiometric division. This assured optimum focussing without readjustment at all electron energies in question.

The electron gun was operated in the energy range 5 to 350 eV and delivered a beam current of several microamperes. The current usually increased with energy. However the current-voltage characteristic could be made rather flat by optimizing the electrode potentials. The electron beam through the collision chamber was well collimated. The current to the collision chamber walls was generally less than 1% of the focussed current monitored at the electron collector (Faraday cup). The energy spread in the beam was about 0.5 eV (FWHM) as determined from the threshold behavior of excitation functions. The beam diameter was about 1 mm and was estimated from the spatial extent of luminosity resulting from electron impact excitation of gases in the collision chamber.

## RESULTS

### OI 1304Å Multiplet

The OI( $2p^4\ ^3P \leftarrow 2p^3\ 3s\ ^3S$ ) transition is the first resonance transition of atomic oxygen and consists of lines at 1302.17, 1304.87, and 1306.04Å.<sup>13</sup> This multiplet was excited by the impact of 100 eV electrons on CO<sub>2</sub> and the spectral region 1280 - 1320Å was scanned at 0.8Å resolution. The closest detectable emission feature to the 1304Å multiplet was the CI 1311Å line. The monochromator was then centered on the OI 1304Å multiplet and the slits were set to yield 6Å resolution. The image of the 1304Å multiplet was included in the unity bandpass region of the monochromator transfer function. The CO<sub>2</sub> pressure in the collision chamber was  $< 2 \times 10^{-4}$  torr and the electron beam current was  $< 2 \times 10^{-5}$  amperes. The emission intensity was earlier found to be linear with pressure and current at these settings. The excitation function was measured and the cross section was later compared to the cross section for dissociative excitation of Lyman alpha (HI 1216Å) radiation by electron impact on H<sub>2</sub>. The absolute cross section for the OI 1304Å multiplet is shown in Fig. 2.

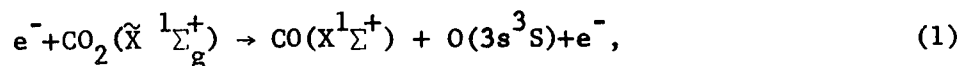
The cross section exhibits an appearance potential at 21 eV  $\pm$  2 eV and a second feature at  $\sim$  45 eV, then rises steeply to a broad maximum centered at 110 eV and then decreases monotonically as the energy increases to 350 eV. The shape of the cross section shows the excitation process is electric dipole allowed at higher energies. The absolute cross section at 100 eV is  $1.0 \times 10^{-18}$  cm<sup>2</sup>  $\pm$  18% (Table II).

The excitation cross sections of Ajello<sup>7</sup> and Sroka<sup>8</sup> are compared

with the results of this work in Figure 3 and Table III. All three curves are in good agreement regarding the appearance potential. There is agreement between Sroka and this work for the position of the second threshold ( $\sim 45$  eV) and between Ajello and this work regarding the position of the peak ( $\sim 110$  eV) and the shape at high energies. The disagreement in shape displayed by Sroka's results at high energies ( $> 100$  eV) may stem from the effects of low energy ( $< 50$  eV) secondary electrons from the collector which are brought back into the collision region by the collimating magnetic field in Sroka's experiment.

It is known that most secondary electrons are low in energy ( $< 50$  eV) with a most probable energy in the range of 1-10 eV.<sup>14</sup> Thus, we expect that the occurrence of shape distortion in a measured excitation function will depend on the threshold value of the excitation process. Processes having thresholds in the neighborhood of 50 eV are expected to show very little shape distortion whereas the distortion should become progressively more pronounced for processes with successively lower thresholds. The shapes which were measured by Sroka and the present authors for the CII 1335 $\text{\AA}$  multiplet (appearance potential  $\sim 45$  eV) are in close agreement (Fig. 9) but the shapes for the OI 1304 $\text{\AA}$  multiplet (appearance potential  $\sim 21$  eV) show a marked disagreement at higher energies. This behavior is consistent with excitation by low energy secondary electrons in Sroka's experiment. The excitation functions presented in Parts I and II of this work exhibit shapes which are in good agreement with the results of other experimenters.<sup>1,2</sup> We have no reason to suspect that the shapes of the excitation functions for  $\text{CO}_2$  are anomalous.

One might at first think that the dissociative process requiring the least energy to make  $O(3s^3S)$  would be

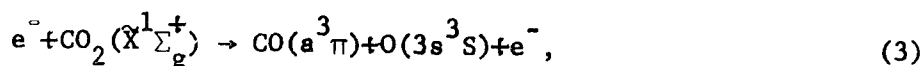


which requires at least 14.97 eV, i.e.

$$T_{\min} = D_o^O(CO-O) + T_e(O^*) \quad (2)$$

$$= 5.45 + 9.52 = 14.97 \text{ eV.}$$

However, correlation rules show that the intermediate  $CO_2^*$  state must be  $^3\Sigma^-$  to yield the fragments shown in eq. 1.<sup>15</sup> Since  $\Sigma^+ \rightarrow \Sigma^-$  transitions are strictly forbidden, eq. 1 does not represent a physically important mechanism.<sup>16</sup> The observed appearance potential is in good agreement with the mechanism (Table IV),



$$T_{\min} = D_o^O(CO-O) + T_e(CO^*) + T_e(O^*)$$

$$= 5.45 + 6.01 + 9.52 = 20.98 \text{ eV.} \quad (4)$$

The  $CO(a^3\Pi)$  state is the lowest triplet state and radiates the Cameron bands in the vacuum ultraviolet.

The second threshold (at 45 eV) probably corresponds to dissociative ionization and excitation following removal of a strongly bonding inner shell electron in  $CO_2$  (see Discussion).



### CI 1329 $\text{\AA}$ Multiplet

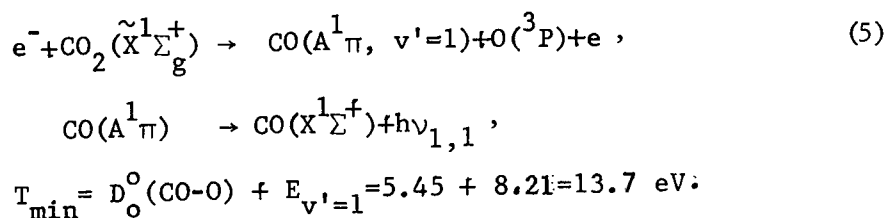
The CI ( $2s^2 2p^2 \ ^3P \leftarrow 2s2p^3 \ ^3P^o$ ) multiplet radiates lines at 1328.82 $\text{\AA}$ , 1329.10 $\text{\AA}$ , and 1329.58 $\text{\AA}$  (Fig. 4).<sup>13</sup> The excitation function for the CI 1329 multiplet was measured at a monochromator bandpass of 4.15  $\text{\AA}$  after first determining that there were no other detectable emission features within this bandpass. The  $\text{CO}_2$  pressure was  $< 5 \times 10^{-4}$  torr and the electron beam current was  $< 2 \times 10^{-5}$  amperes. The excitation function was put on an absolute scale at 100 eV by comparing it to the OI 1304 $\text{\AA}$  cross section which was described in the previous section (Table II). The absolute excitation cross section for the CI 1329 multiplet is shown in Fig. 5. The appearance potential ( $\sim 24$  eV) is only approximate since the counting statistics were poor ( $\sim 10\%$  at the peak). The observed appearance potential is compared to possible sets of states for the fragment species in Table IV.

The cross section rises steeply from threshold to a broad maximum centered at 100 eV (Table II) and then decreases monotonically at higher energies. The shape is characteristic of an electric - dipole-allowed process. The scatter in the data is too great to determine whether there is a second threshold at  $\sim 45$  eV.

### CI 1561 $\text{\AA}$ Multiplet

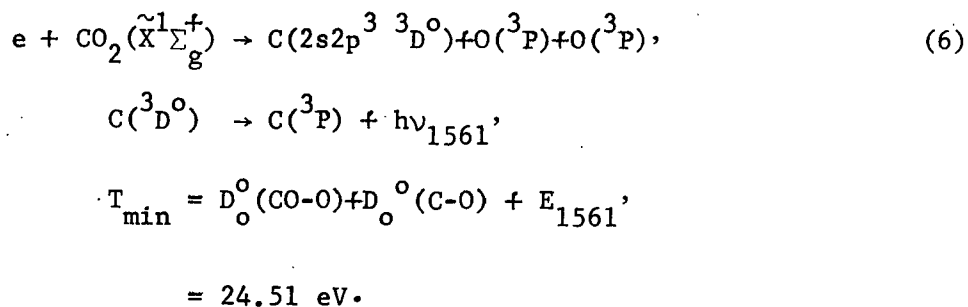
The CI ( $2s^2 2p^2 \ ^3P \leftarrow 2s2p^3 \ ^3D^o$ ) multiplet radiates lines at 1560.31, 1560.70, 1561.29, and 1561.40 $\text{\AA}$  (Fig. 4).<sup>13</sup> The CI 1561 multiplet was overlapped by the (1,1) and (4,3) bands of the CO fourth positive system which was excited by dissociative excitation of  $\text{CO}_2$ . The bandheads lie at 1560 $\text{\AA}$  and the bands are degraded to longer wavelengths

so that they overlap the entire multiplet. An excitation function was measured at 12Å resolution for the sum of the (1,1) band, the (4,3) band, and the CI 1561Å multiplet (Fig. 6). The measured appearance potential corresponds to the threshold for dissociative excitation to the  $v'=1$  vibrational level of the  $\text{CO}(A^1_\pi)$  state, i.e.



The shape of the excitation function of the (1,1) band has been reported elsewhere<sup>3</sup> and is shown by the dashed line in Fig. 6. The (4,3) band is only 1/10 as intense as the (1,1).

A second threshold occurs at ~26 eV and can tentatively be identified with the total dissociation process (Table IV)



The cross section rises steeply through a subsidiary maximum at ~38 eV to a third threshold at ~46 eV after which it rises to a broad maximum centered at 105 eV. The structure at 46 eV probably

represents dissociative ionization by removal of an inner shell electron from the  $3\sigma_g$  orbital of  $\text{CO}_2$  (see Discussion). The absolute total cross section (bands + multiplet) was determined at 100 eV by comparing with the OI 1304 cross section and was found to be  $9.7 \times 10^{-19} \text{ cm}^2 \pm 22\%$  of which  $7.5 \times 10^{-19} \text{ cm}^2$  was due to the CI 1561 multiplet (Table II). The shape of the cross section at high energies is characteristic of an electric dipole allowed transition.

#### CI 1657 $\text{\AA}$ Multiplet

The CI ( $2p^2\ ^3P \leftarrow 2p3s\ ^3P^0$ ) multiplet consists of lines at 1656.26, 1656.92, 1657.00, 1657.37, 1657.89, and 1658.11 $\text{\AA}$  (Fig. 4).<sup>13</sup> The CI 1657 multiplet was overlapped by the (0,2) band of the CO fourth positive system which was excited by dissociative excitation of  $\text{CO}_2$ . The excitation function for the sum of the (0,2) band and the CI 1657 multiplet was measured at 16.6 $\text{\AA}$  resolution (Fig. 7). The appearance potential was  $14 \text{ eV} \pm 2 \text{ eV}$  in good agreement with the expected threshold (13.53 eV) for excitation of  $\text{CO}(A^1\pi, v'=0)$  by the mechanism of eq. 5. The shape of the excitation cross section for the CO  $4^+$  (1,1) band has been reported elsewhere<sup>3</sup> and is shown by the dashed line in Fig. 7. A second threshold occurs at  $\sim 25 \text{ eV}$ . This is consistent with production of the CI 1657 multiplet by a mechanism leading to total dissociation (Table IV) which requires at least 24.06 eV of energy (neglecting kinetic energy of the dissociation fragments). A third threshold occurs at  $\sim 50 \text{ eV}$  and probably corresponds to dissociative ionization and excitation. The cross section rises to a broad maximum centered at  $\sim 110 \text{ eV}$  and thereafter decreases with increasing energy. The shape is characteristic of an electric-dipole-allowed transition. The

value of the total cross section at 100 eV is  $1.5 \times 10^{-18} \text{ cm}^2 \pm 22\%$  of which  $1.4 \times 10^{-18} \text{ cm}^2$  is due to the CI 1657 multiplet.

#### CII 1335 Å Multiplet

The CII ( $2s^2 2p^2 \text{ } ^2\text{P}^0 \leftarrow 2s 2p^2 \text{ } ^2\text{D}$ ) multiplet consists of lines at 1334.53, 1335.66, and 1335.71 Å (Fig. 4).<sup>13</sup> The excitation function (Fig. 8) was measured at 4.15 Å resolution and no other emission features were detected in this bandpass. The appearance potential is  $44 \pm 2$  eV and is compared to possible states of the dissociation fragments in Table IV. There are many possible sets of states which have  $T_{\text{min}} < 44$  eV. The excess energy may be stored in the electronic structure of the oxygen atoms or may appear as kinetic energy. It cannot represent a cascade mechanism in the CII ion since the emission cross section of the CII 1324 multiplet was found to be less than 2% of the CII 1335 cross section at 100 eV (Table II). The CII 1335 cross section rises smoothly from threshold to a broad maximum which is centered at  $\sim 170$  eV and then decreases monotonically at higher energies. The absolute value at 100 eV is  $7.6 \times 10^{-19} \text{ cm}^2 \pm 23\%$  (Table II) and the shape is characteristic of an electric-dipole-allowed transition.

The present data are compared with the data of Ajello<sup>7</sup> and Sroka<sup>8</sup> in Fig. 9 and Table V. The shapes are in good agreement but Sroka's absolute values differ by about a factor of two from Ajello's. Ajello's work and the present results are the preferred values since these experimenters utilized recently developed calibration techniques which enable accurate calibration of monochromators over the wavelength range 1100 - 2600 Å.

## DISCUSSION

In this paper we have presented excitation cross sections (5 - 350eV) for multiplets of OI, CI, and CII by electron impact on CO<sub>2</sub>. All of the observed excitation processes were electric-dipole-allowed at high energies. The OI 1304<sup>8</sup>Å multiplet exhibits an appearance potential corresponding to the fragments CO and O. The CI and CII multiplets exhibit appearance potentials which are larger by several volts (~5) than the lowest possible energy for producing C + O<sub>2</sub> or C<sup>+</sup> + O<sub>2</sub>, respectively. Thus, if O<sub>2</sub> is a direct dissociation fragment, there is ~5 eV available for distribution among the fragments. The close agreement between the excess energy and the bond energy of O<sub>2</sub> suggests that the CO<sub>2</sub> fragments completely. The excitation functions for the OI and CI multiplets exhibit secondary thresholds at ~45 eV while the CII 1335 multiplet exhibits an appearance potential at ~44 eV. This strongly suggests that these secondary thresholds and the CII appearance potential represent dissociative excitation or ionization involving excitation of a strongly bonding electron from an inner shell orbital of CO<sub>2</sub>. This hypothesis is supported by the known characteristics of the molecular orbitals of CO<sub>2</sub>.

The ground configuration of CO<sub>2</sub> may be written,

$$\text{CO}_2 (\tilde{X}^1\Sigma_g^+) (1\sigma_g)^2 (1\sigma_u)^2 (2\sigma_g)^2 (3\sigma_g)^2 (2\sigma_u)^2 (4\sigma_g)^2 (3\sigma_u)^2 (1\pi_u)^4 (1\pi_g)^4. \quad (7)$$

The outer shell electrons have vertical ionization potentials of 13.8, 17.6, 18.1, and 19.4 eV, corresponding to removal of an electron from the 1 $\pi_g$ , 1 $\pi_u$ , 3 $\sigma_u$ , and 4 $\sigma_g$  orbitals, respectively<sup>17</sup> (Table VI).

All of the multiplets observed in this work have appearance potentials which are greater than the first four ionization limits. The location of the next ionization limits have been estimated by various authors.<sup>18,19,20</sup>

The most complete calculation (McLean and Yoshimina) predicts orbital energies of 40.2 eV and 41.6 eV for  $1\sigma_u$  and  $3\sigma_g$  orbitals, respectively. These calculated values are quoted to the third figure to indicate the internal accuracy of the calculation. The calculated orbital energies bear only an approximate relation to the actual ionization limits. This may best be seen by comparing the calculated orbital energies with the observed values for the adiabatic ionization limits of the four outer orbital (Table IV) which differ by  $\sim 10 - 15\%$ . Thus the calculated orbital energies should be viewed as approximations to their respective ionization limits. The ionization limits can best be determined by experiment.

Measurements of the photoelectron spectrum of  $\text{CO}_2$  have shown that the  $1\pi_g$ ,  $3\sigma_u$ , and  $4\sigma_g$  orbitals are non-bonding while the  $1\pi_u$  orbital is strongly bonding in character.<sup>17</sup> These results confirmed the calculations of Peyerimhoff et al.<sup>19</sup> and showed that Mulliken's<sup>21</sup> original classification of the bonding character of the  $\sigma$  - type orbitals was incorrect. Peyerimhoff's results also showed that the orbitals ( $2\sigma_g$ ,  $1\sigma_u$ ,  $1\sigma_g$ ) may be regarded as atomic orbitals ( $1s_c$ ,  $1s_o$ ,  $1s_o$ ) and are very tightly bound, playing no further role in this discussion. The  $2\sigma_u$  orbital is composed primarily of ( $2s_o - 2s_o$ ) character and removal of an electron from this orbital will result in an excited oxygen ion if the core  $\text{CO}_2^+$  dissociates. The  $3\sigma_g$  orbital can be written ( $2s_o + 2s_c + 2s_o$ ) and dissociation following removal of an electron from the  $3\sigma_g$  orbital will have a certain probability of producing a carbon ion with the configuration  $\text{CII}(1s^2 2s 2p^2)$ .

We have observed production of this state (i.e. we observed the CII 1335 $\text{\AA}$  multiplet) and found the appearance potential to be  $\sim 44$  eV. The three independent measurements of the appearance potential are in agreement with a value of 45 eV (Table V). We conclude that the CII 1335 $\text{\AA}$  multiplet is produced by removal of an electron from the  $3\sigma_g$  orbital accompanied by dissociation of the core ion. The appearance potential is a direct measure of the vertical ionization potential of the  $3\sigma_g$  orbital (45 eV).

Since the  $3\sigma_g$  orbital is composed of a linear combination of atomic orbitals ( $2s_o$ ,  $2s_c$ , and  $2s_o$ ) we expect that removal of an electron from that orbital will have a certain probability to produce  $\text{OII}(1s^2 2s 2p^4) + \text{OI} + \text{CI}$ . Thus one expects to find radiation at 833.8 $\text{\AA}$   $\text{OII}(2s^2 2p^3 \leftarrow 2s 2p^4)$  with an appearance potential at  $\sim 45$  eV or less, depending on whether dissociative ionization from the  $2\sigma_u$  orbital also occurs. Sroka<sup>8</sup> observed an appearance potential of  $\sim 48$  eV for this multiplet which suggests that only the  $3\sigma_g$  orbital is involved near threshold.

The observed appearance potentials for the CI multiplets fall in the range 24-26 eV (Table IV). These processes must represent dissociative excitation through doubly excited valence states or doubly excited Rydberg states of  $\text{CO}_2$  rather than through singly excited Rydberg states belonging to the known ionization limits since the Rydbergs of a given series lie within  $\sim 4$  eV of the ionization limit.<sup>22</sup> There are no singly excited Rydberg states between  $\sim 19.4$  eV and  $\sim 38$  eV. A glance at the CI term diagram (Fig. 4) shows that the CI 1657 $\text{\AA}$  multiplet

originates through a doubly excited Rydberg state of  $\text{CO}_2$  whereas the  $\text{CI } 1561\text{\AA}^0$  multiplet probably originates through a doubly excited valence state.

It should also be noted that the  $\text{OI}(2p^3 3s)$  configuration is a Rydberg state of oxygen. This implies that the intermediate state of  $\text{CO}_2$  (which dissociates according to eq. 1 and leads to emission of the  $\text{OI } 1304\text{\AA}^0$  multiplet) is also a Rydberg. This Rydberg of  $\text{CO}_2$  must be doubly excited since it lies  $\sim 21$  eV above the ground state.

Thus, the observed multiplets represent two kinds of processes; (1) single electron excitation from inner shell orbitals and (2) double electron excitation from outer shell orbitals. Dissociative excitation following single electron excitation from outer shell orbitals has not been observed in this work. However, this process does lead to production of  $\text{CO}(\text{A}^1_\pi)$  and  $\text{CO}(\text{a}^3_\pi)$  which results in emission of the fourth positive band system and the Cameron band system, respectively.<sup>3,7,23</sup>

## CONCLUSION

In this series of papers we have described absolute cross sections for dissociative excitation of  $\text{H}_2$ ,  $\text{O}_2$ ,  $\text{N}_2$ ,  $\text{CO}_2$ , and  $\text{CO}$  by electron impact to yield vacuum ultraviolet features in the wavelength range  $1165 - 1900\text{\AA}^0$ . These data were needed for calculations of the primary production rates of these features by secondary electrons in disturbed planetary atmospheres<sup>24</sup> (aurora) and by photoelectrons in the dayglows of Mars and Venus.<sup>6</sup> In addition to the practical applications of these results, they provide insight for better understanding the phenomena of molecular dissociation and demonstrate the need for careful experimental probing of molecular states (stable and unstable) above the first ionization limit.



# ACKNOWLEDGMENT

We wish to thank Dr. M. Krauss for stimulating discussions and for reading the manuscript. The assistance of Dr. Edward Stone in the data taking is gratefully acknowledged.

## FOOTNOTES AND REFERENCES

\*This research was supported by the Advanced Research Project Agency, The Department of Defense, and was monitored under Contract No. DA-31-124-ARO-D-440 and by the National Aeronautics and Space Administration (NGL 39-011-030).

<sup>+</sup>Preliminary results of this work were presented at the 22nd Gaseous Electronic Conference (27-31 October 1969), Gatlinburg, Tennessee [Bull. Am. Phys. Soc. 15, 422 (1970)].

<sup>‡</sup> Present Address: Astrochemistry Branch, Code 691, Laboratory for Extraterrestrial Physics, NASA/Goddard Space Flight Center, Greenbelt, Maryland 20771.

<sup>\*\*</sup> Present Address: Department of Physics, Southern Illinois University, Carbondale, Illinois 62901.

1. M. J. Mumma and E. C. Zipf, J. Chem. Phys. 55, 1661 (1971).
2. M. J. Mumma and E. C. Zipf, J. Chem. Phys. 55, 5582 (1971).
3. M. J. Mumma, E. J. Stone, and E. C. Zipf, J. Chem. Phys. 54, 2627 (1971).
4. M. J. Mumma, E. J. Stone, and E. C. Zipf, Abstracts VIIth Intl. Conf. Physics of Electronic and Atomic Collisions, (North-Holland), 858 (1971).
5. C. A. Barth, C. W. Hord, J. B. Pearce, K. K. Kelly, G. P. Anderson, and A. I. Stewart, J. Geophys. Res. 76, 2213 (1971).
6. M. B. McElroy and J. C. McConnell, J. Geophys. Res. 76, 6674 (1971).
7. J. Ajello, J. Chem. Phys. 55, 3169 (1971).
8. W. Sroka, Z. Naturforsch. 25a, 1434 (1970).
9. M. J. Mumma, Dissociative Excitation of Atmospheric Gases, Ph.D. Thesis, University of Pittsburgh (1970).
10. M. J. Mumma and E. C. Zipf, J. Opt. Soc. Am. 61, 83 (1971).
11. A similar electron gun was briefly described by W. L. Borst and E. C. Zipf, Phys. Rev. 1, 834 (1970). A more detailed description is presented in this paper.
12. J. A. Simpson and C. E. Kuyatt, Rev. Sci. Instr. 34, 265 (1963).
13. W. L. Wiese, M. W. Smith, and B. M. Glennon, Natl. Std. Ref. Data. Ser. Natl. Bur. Std. (U.S.) Vol. 1 (1966).

14. N. R. Whitten, in "Methods of Experimental Physics, Vol. 4, Part A" ed. L. Marton (Academic Press, London, 1967), p. 69.
15. G. Herzberg, Molecular Spectra and Molecular Structure Vol. III, 2d ed. (Van Nostrand, 1950), p. 283.
16. D. C. Cartwright, S. Trajmar, W. Williams, D. L. Huestis, Phys. Rev. Letters 27, 704(1971).
17. C. R. Brundle and D. W. Turner, Intl. J. Mass Spectrom. and Ion Phys. 2, 195 (1969).
18. J. F. Mulligan, J. Chem. Phys. 19, 347(1951).
19. S. D. Peyerimhoff, R. J. Buenker, and J. L. Whitten, J. Chem. Phys. 46, 1707(1967).
20. A. D. McLean and M. Yoshimina, "Tables of Linear Molecule Wave Functions," IBM Report, San Jose Research Laboratory, International Business Machines Corporation, San Jose, Calif(1967).
21. R. S. Mulliken, J. Chem. Phys. 3, 720(1935).
22. By "doubly-excited valence state" we mean a state which has two occupied valence orbitals which are excited with respect to the  $\text{CO}_2(\tilde{X}^1\Sigma_g^+)$  ground state configuration. Similarly, "doubly excited Rydberg state" means a state having one occupied valence orbital and one occupied Rydberg orbital which are excited with respect to the ground state configuration.
23. M. Krauss, S. R. Mielczarek, D. Neumann, C. E. Kuyatt, J. Geophys. Res. 76, 3733 (1971).
24. E. C. Zipf and E. J. Stone, J. Geophys. Res. 76, 6865(1971).

## LIST OF FIGURES

- Fig. 1. Schematic diagram of the electron gun showing the filament (F), grid (G), anode (A), lens (L), final electrode (P), and the apertures ( $d_1$ ,  $d_2$ ,  $d_3$ ,  $d_4$ ,  $d_5$ ).
- Fig. 2. Absolute cross section for dissociative excitation of the OI 1304 Å resonance multiplet by electron impact on CO<sub>2</sub>. The solid curve represents the smoothed data.
- Fig. 3. Absolute cross section for dissociative excitation of the OI 1304 Å resonance multiplet by electron impact on CO<sub>2</sub>: --- Ajello, ---- Sroka, — present results.
- Fig. 4. Partial term level diagram of CI and CII showing the multiplets observed in this work.
- Fig. 5. Absolute cross section for dissociative excitation of the CI 1329 Å multiplet by electron impact on CO<sub>2</sub>. The solid curve represents the smoothed data.
- Fig. 6. Absolute cross section for dissociative excitation of the CI 1561 Å multiplet by electron impact on CO<sub>2</sub>. The dashed curve represents the contribution of the (1,1) vibrational band of the CO fourth positive group. The solid curve represents the smoothed data.
- Fig. 7. Absolute cross section for dissociative excitation of the CI 1657 Å multiplet by electron impact on CO<sub>2</sub>. The dashed curve represents the contribution of the (0,2) vibrational band of the CO fourth positive group. The solid curve represents the smoothed data.

Fig. 8. Absolute cross section for dissociative excitation of the CII 1335 Å multiplet by electron impact on CO<sub>2</sub>. The solid line represents the smoothed data.

Fig. 9. Comparison of cross sections measured for dissociative excitation of the CII 1335 Å multiplet by electron impact on CO<sub>2</sub>: ----- Ajello, ----- Sroka, ----- present results.

TABLE I. ELECTRON GUN PARAMETERS\*

Electrode	Potential	Aperture diameter (mm)
Filament F	- $V_0$	
Grid G	- $0.6 V_0$	$d_1 = 1.5$
Anode A	+ $4.3 V_0$	$d_2 = 1.5$
		$d_3 = 6.3$
Electrode L	+ $4.3 V_0$	
Decelerator P	0	$d_4 = 6.3$
Collision Chamber	0	$d_5 = 3.2$
Electron Collector	+ 15 volt	

\* See also Fig. 1 and text.

TABLE II. ABSOLUTE EMISSION CROSS SECTIONS  
FOR MULTIPLETS OF OI, CI, AND CII PRODUCED BY ELECTRON  
IMPACT (100 eV) ON CO<sub>2</sub>.

	This work	Ajello	Sroka
OI 1304 Å	* 1.04(-18) ± 18%	* 7.56(-19)±30%	*5.7(-19)
CI 1329 Å	* 2.67(-19) ± 21%	2.50(-19)	--
CI 1561 Å	* 7.50(-19) ± 30%	6.79(-19)	--
CI 1657 Å	* 1.45(-18) ± 23%	1.31(-18)	--
CII 1324 Å	1.33(-20) ± 23%	---	---
CII 1335	* 7.60(-19) ± 22%	* 7.6(-19)	*8.8(-19)

\* = excitation function presented.



TABLE III. COMPARISON OF RESULTS FOR THE OI 1304 Å  
MULTIPLY

	This Work	Ajello <sup>a</sup>	Sroka <sup>b</sup>
Threshold	21 ± 2	21 ± 2	21.5
2nd Threshold	~45	35	~45
peak	~110	100	160-175

a. Ref. 7.

b. Ref. 8.

TABLE IV

Appearance Potentials for Atomic VUV Emission Features  
Produced by Dissociative Excitation of CO<sub>2</sub>.

Multiplet	Possible configuration of Dissociation Fragments	Minimum Appearance Potential, eV	
		Theoretical	Observed
OI 1304 <sup>0</sup>	OI(3s <sup>3</sup> S) + CO(A <sup>1</sup> π),	23.00	
	OI(3s <sup>3</sup> S) + CO(B <sup>3</sup> π)	20.98	21
	OI(3p <sup>3</sup> P) + CO(X <sup>1</sup> Σ <sup>+</sup> )	16.48 (a)	
	OI(3s <sup>3</sup> S) + CO(X <sup>1</sup> Σ <sup>+</sup> )	14.97 (b)	
CI 1329 <sup>0</sup>	CI(2s2p <sup>3</sup> <sup>3</sup> P <sup>o</sup> ) + 2OI(2p <sup>4</sup> <sup>3</sup> P)	25.90	24
	CI(2s2p <sup>3</sup> <sup>3</sup> P <sup>o</sup> ) + O <sub>2</sub> (X <sup>3</sup> Σ <sub>g</sub> <sup>-</sup> )	20.82	
CI 1561 <sup>0</sup>	CI(2s2p <sup>3</sup> <sup>3</sup> D <sup>o</sup> ) + 2OI(2p <sup>4</sup> <sup>3</sup> P)	24.51	~26
	CI(2s2p <sup>3</sup> <sup>3</sup> D <sup>o</sup> ) + O <sub>2</sub> (X <sup>3</sup> Σ <sub>g</sub> <sup>-</sup> )	19.43	
CI 1657	CI(3s <sup>3</sup> P <sup>o</sup> ) + 2 OI(2p <sup>4</sup> <sup>3</sup> P)	24.05	~25
	CI(3s <sup>3</sup> P <sup>o</sup> ) + O <sub>2</sub> ( <sup>3</sup> Σ <sub>g</sub> <sup>-</sup> )	18.97	
CII 1335 <sup>0</sup>	CII(2s2p <sup>2</sup> <sup>2</sup> D) + 2 OI(2p <sup>4</sup> <sup>3</sup> P)	37.11	~44
	CII(2s2p <sup>2</sup> <sup>2</sup> D) + OI(2p <sup>4</sup> <sup>1</sup> D) + OI(2p <sup>4</sup> <sup>3</sup> P)	39.07	
	CII(2s2p <sup>2</sup> <sup>2</sup> D) + 2OI(2p <sup>4</sup> <sup>1</sup> D)	41.03	
	CII(2s2p <sup>2</sup> <sup>2</sup> D) + OI(2p <sup>4</sup> <sup>1</sup> S) + OI(2p <sup>4</sup> <sup>3</sup> P)	41.30	
	CII(2s2p <sup>2</sup> <sup>2</sup> D) + OI(2p <sup>4</sup> <sup>1</sup> S) + OI(2p <sup>4</sup> <sup>1</sup> D)	43.26	
	CII(2s2p <sup>2</sup> <sup>2</sup> D) + 2OI(2p <sup>4</sup> <sup>1</sup> S)	45.47	

- a. The OI(2p <sup>3</sup>P) cascades to OI(3s <sup>3</sup>S) through emission of a photon at 8447<sup>0</sup>Å. In one very good data run we saw a feature which had a threshold at ~16 eV and a cross section of ~1x10<sup>-20</sup> cm<sup>2</sup>. The shape seemed to peak near threshold. We have not included this feature in Fig. 2 since we had trouble reproducing the observation.
- b. This combination of final states can arise only from a Σ<sup>-</sup> intermediate CO<sub>2</sub><sup>\*</sup> state. We can therefore exclude this set of final states since Σ<sup>+</sup> → Σ<sup>-</sup> transitions are forbidden by electric dipole interaction.

TABLE V

A COMPARISON OF SALIENT FEATURES OF THE CII 1335 Å  
CROSS SECTION.

	This Work	Ajello <sup>a</sup>	Sroka <sup>b</sup>
Threshold	~44 eV	~45 eV	~45 eV
Peak	~175 eV	~170 eV	~170 eV
$\sigma(170 \text{ eV})$	$10.0(-19)\text{cm}^2$	$8.3(-19)\text{cm}^2$	$13.5(-19)\text{cm}^2$

a. Ref. 7.

b. Ref. 8.

TABLE VI. ORBITAL ENERGIES AND IONIZATION POTENTIALS OF CO<sub>2</sub>

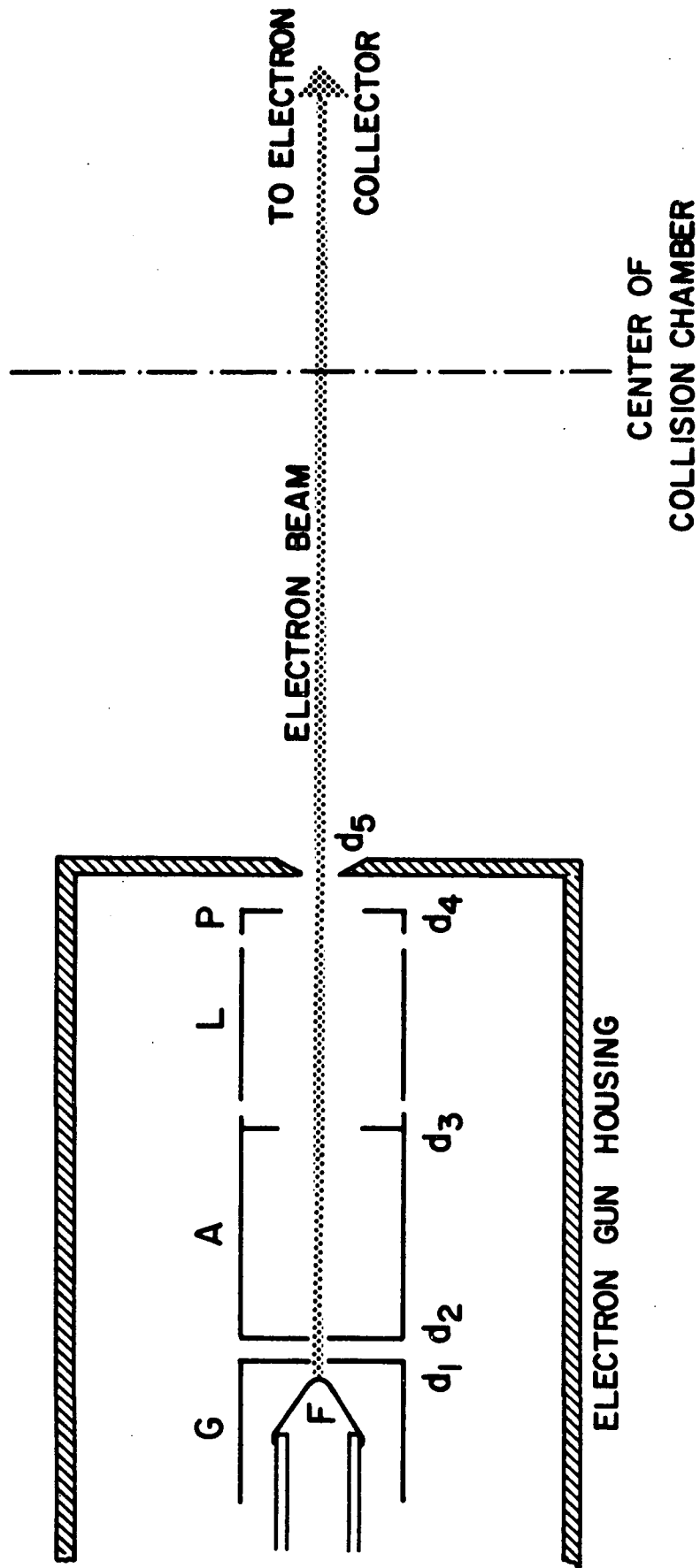
Orbital	Orbital Energy		Ionization Potential
1 $\pi_g$	14.7 <sup>a</sup> , 14.7 <sup>b</sup>		13.8
1 $\pi_u$	20.1 <sup>a</sup> , 18.9 <sup>b</sup>		17.6 <sup>c</sup>
3 $\sigma_u$	19.5 <sup>a</sup> , 19.9 <sup>b</sup>		18.1
4 $\sigma_g$	21.4 <sup>a</sup> , 21.9 <sup>b</sup>		19.4
2 $\sigma_u$	41.0 <sup>a</sup> , 40.2 <sup>b</sup>		
3 $\sigma_g$	42.7 <sup>a</sup> , 41.6 <sup>b</sup>		(45) <sup>d</sup>

a. Ref. 19

b. Ref. 20

c. Vertical Ionization Potential.

d. Vertical Ionization Potential determined in the present work.



1 INCH

